Check for updates

ChemCatChem

ChemCatChem
Chemistry Europe
European Chemical Societies Publishing

RESEARCH ARTICLE OPEN ACCESS

From Structure to Stability: A Comparative Evaluation of Ammonium- and Phosphonium-Based Deep Eutectic Solvent Catalysts in Glycerolysis

Kapil Mamtani[1] | Mohammed Mehdi Farid[1] | Kaveh Shahbaz[2]

[1]Department of Chemical and Materials Engineering, The University of Auckland, Auckland, New Zealand | [2]College of Science and Engineering, James Cook University, Townsville, Queensland, Australia

Correspondence: Kapil Mamtani (kmam238@aucklanduni.ac.nz)

Received: 17 January 2026 | **Revised:** 4 May 2026 | **Accepted:** 22 May 2026

Keywords: acidic deep eutectic solvents | catalyst recyclability | hydrogen-bond network | water tolerance

ABSTRACT

Deep eutectic solvents (DESs) are efficient catalysts; however, their foundational hydrogen-bonding framework is susceptible to water-induced disruptions. In this study, a structure-stability-performance relationship is examined for two acidic DESs: tetrabutylammonium hydrogensulfate (N-DES) and tetraphenylphosphonium bromide (P-DES) with p-toluenesulfonic acid monohydrate (PTSAM), in a glycerolysis reaction. Glycerolysis of free fatty acids (FFAs) generates water as by-product, creating dynamic water-rich reaction environment, providing a controlled basis for comparing two DESs against water-ingression. N-DES being more acidic achieved equilibrium conversion faster than P-DES, under identical conditions, validated by lower apparent activation energy for N-DES. Both DESs remained in the glycerol phase post-reaction, and under recycle routine there was water build-up in glycerol phase. The water ingress affected the catalytic stability of both DESs, while removing water via oven evaporation, resulted in improved catalytic conversion- N-DES (40% to 62%) in comparison to P-DES (46% to 81%), at the end of fifth cycle. TGA data confirms thermal stability of both DESs within operational ranges, eliminating DES degradation behind decreased catalytic ability. Insights from viscosity and molecular self-diffusion data highlights the differences in component mobility and hydrogen-bond network organization, as most probable cause of divergent resistance to water-induced disruption during recycling.

1 | Introduction

Industrial or waste-derived nonedible lipid sources, often containing high levels of free fatty acids (FFAs) are promising feedstock for sustainable production of fuels and materials [1, 2]. Biodiesel, a petro–diesel substitute, commonly known as fatty acid methyl esters (FAMEs), is commercially produced via methanolic transesterification of triglycerides in neat vegetable oils [3, 4]. However, FAMEs conversion is sensitive to high FFAs content, where FFAs react with alkaline catalysts to form soaps, which lowers yield and causes emulsification [5]. Glycerolysis or glycerol esterification of FFAs provides a chemical route to convert FFA-rich residues into glycerides that re-enter conventional transesterification pathways [6]. Transesterification by-product, glycerol has three hydroxyl groups and is a highly hydrophilic molecule, it exhibits limited solubility in organic media; for instance, glycerol is soluble only up to 4%–5% in typical hydrophobic fats. This low solubility hinders the reaction unless it is carried out at elevated temperatures or in the presence of an effective catalyst to assist glycerol (a weak nucleophile). Deep eutectic solvents (DESs) have emerged as versatile media and catalysts for acid-catalyzed transformations, owing to their tunable hydrogen-bond networks, low toxicity, and recyclability [7–9]. Unlike Ionic Liquids, DESs have simpler synthesis routine, rather

This is an open access article under the terms of the Creative Commons Attribution License, which permits use, distribution and reproduction in any medium, provided the original work is properly cited.
© 2026 The Author(s). *ChemCatChem* published by Wiley-VCH GmbH

cost-effective components, while retaining low-volatility [10]. However, the fundamental hydrogen bonding governing DESs structure is susceptible to water ingression, significantly affecting the reaction equilibria and catalyst stability [11]. Furthermore, the physicochemical behavior of DESs in solvolysis or catalysis is governed by the complex hydrogen-bonding interactions, which are dependent on component-specific associations [12].

Acidic DESs based on quaternary salts and organic acid have been reported earlier by Mamtani et al. (2023)- tetrabutylammonium hydrogensulfate (N-DES) and tetraphenylphosphonium bromide (P-DES) with p-toluenesulfonic acid monohydrate (PTSAM), respectively [13]. Advanced characterization quantified physicochemical properties of two DESs, establishing thermal behavior, ionicity, viscosity, conductivity and molecular diffusion trends. The group then investigated application of N-DES in glycerolysis of FFAs, reporting high catalytic activity but poor catalyst recyclability (conversion falling to ≈ 62.5% after five cycles and reduced conversion when using crude glycerol), owing to water, a reaction by-product [14]. Lower catalyst recyclability was hypothesized to arise from water-based disruption of N-DES structure. In P-DES, the HBA is composed of an aromatic cation with increased charge delocalization, which may reduce effecting coupling of HBA cation and HBD complex, as observed from previous ^{1}H-NMR self-diffusion data- partial decoupling of the hydrogen-bond donor from the ionic framework in the phosphonium-based DES.

Considering combined evidence establishing structure-property-performance relationship, arising from reported studies, it is hypothesized that substituting ammonium cation in HBA with aromatic phosphonium cation, may lead to a more durable DES structure with moderated interactions with water, thereby resisting water-induced structural disruptions and thus improving catalyst recyclability. Hence, the present study investigates P-DES in glycerolysis of FFAs for its catalytic performance, especially catalyst recyclability. The focus of work is not reaction optimization or catalyst screening, but reaction kinetics and associated parameters are examined to contextualize stability related performance differences relative to N-DES (considered as benchmark). Special emphasis is placed on catalyst reusability and performance under water-rich conditions, as these aspects directly reflect structural stability of the DES catalyst during repeated glycerolysis cycles.

2 | Experimental Section

2.1 | Materials

Table S1 shows the list of chemical reagents used in this research study. All the chemicals were used as received without any modification. Oleic acid was used as model FFA.

2.2 | Catalyst Preparation

The acidic DESs investigated in this study comprise a quaternary salt as hydrogen bond acceptors (HBAs- N-DES or P-DES), both formed using p-toluene sulfonic acid monohydrate (PTSAM) as the hydrogen bond donor (HBD). These catalysts differ only in the hydrogen-bond acceptor framework, enabling a controlled comparison of ammonium and phosphonium systems under identical glycerolysis conditions. Briefly, P-DES was prepared using the standard heating-mixing method described elsewhere [15]. The corresponding ammonium-based DES (N-DES), used as the benchmark catalyst in this study, has been described in detail and applied in glycerolysis of FFAs in our earlier work [14].

Comprehensive physicochemical characterization of both DES catalysts, including acidity, thermal behavior, density, viscosity, and water content, has been reported elsewhere [13] and is not repeated here. Key physicochemical properties relevant to catalytic performance, including Hammett acidity, melting behavior, density, viscosity, and water content, are tabulated below in Table 1.

TGA mass change values reflect overall volatility and loss of weakly associated species and do not indicate catalyst decomposition within the operable temperature range.

2.3 | Reaction Setup and Glycerolysis Procedure

A batch reactor was employed made up of a stainless-steel vessel (250 mL) fitted with an axial impeller, temperature probe, and reactor lid that had an opening for sampling, and nitrogen purging. Heating was provided with a hot plate (fitted with a temperature controller device), insulation provided to minimize heat losses, and purging was provided using flow meter maintained at 80–120 mL/min rate. Moisture in the effluent nitrogen was condensed using a pair of condensers; one hot maintained at 60°C and other cold maintained at room temperature. Oleic acid and pure glycerol were used as model reactants for purpose of establishing reaction kinetics. Both reactants and catalyst were heated to the desired temperature separately and then mixed, marking the beginning of the reaction. The reaction progress was tracked by sampling at the marked time intervals of 0, 5, 10, 15, 30, 45, 60, 90, 120, 150, and 180 min. The 5 mL samples were withdrawn from the reactor and immediately quenched with ice to stop any reaction. The conversion of FFAs was calculated as the average of two independently repeated runs for each experimental condition.

2.4 | Product Analysis

After the glycerolysis reaction and ice-quenching, the products consisted of an upper layer (i.e., mono-, di-, tri-glycerides, and unreacted oleic acid) and a lower layer (i.e., excess glycerol and water). The upper layer was analyzed for composition. The oleic acid (FFA) content was determined by the Lubrizol method for commercial fats and oils [16]. Glyceride composition was determined by gas chromatography with flame ionization detection (GC-FID) using calibrated monoolein and diolein standards, while water content was measured using Karl Fischer coulometric titration. All analyses were performed in duplicate, and the resulting conversions and compositions were reported as average values. Detailed analytical procedures, calibration methods, and calculation steps are provided in Supporting Information.

18673899, 2026, 11, Downloaded from https://chemistry-europe.onlinelibrary.wiley.com/doi/10.1002/cctc.70844 by James Cook University, Wiley Online Library on [10/11/2026]. See the Terms and Conditions (https://onlinelibrary.wiley.com/terms-and-conditions) on Wiley Online Library for rules of use; OA articles are governed by the applicable Creative Commons License

TABLE 1 | Important properties of quaternary acidic N-DES and P-DES, reproduced from [13].

	Molar mass (g/mol)	Melting point	Water content	Mass change	Mass Density	Dynamic viscosity	H_0 [a]
N-DES	719.94	−43.18°C	4.50%	1.75% (25°C–130°C)	1.125 g/cm^3 (at 90°C)	0.055 Pa s (at 90°C)	−2.91
P-DES	247.49	64.30°C	4.37%	9.81% (25°C–135°C)	1.271 g/cm^3 (at 90°C)	0.181 Pa-s (at 90°C)	−1.89

[a] H_0 represents Hammett acidity value in 40 mM aqueous solution.

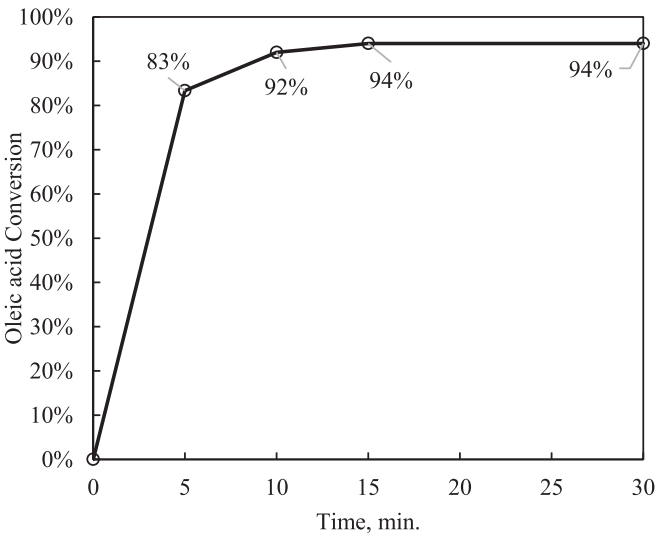


FIGURE 1 | Oleic acid conversion in the glycerolysis reaction using P-DES catalyst at optimum conditions: 130°C and 10 wt.% catalyst loading.

3 | Results and Discussion

3.1 | Glycerolysis of Oleic Acid

Glycerolysis of oleic acid using the phosphonium-based DES (P-DES) catalyst was investigated over a range of temperatures (90°C–150°C) and catalyst loadings (1–10 wt.%), with the parameter range selected to match conditions previously established for ammonium-based DES systems, discussed in Section S3.1 [17]. The experimental parameter range for optimization study were identical with N-DES work, to enable a direct comparison. Figure 1 (and Figure S2) shows oleic acid conversion trend, achieving equilibrium conversion (94%) within 15 min at 130°C with catalyst loading (10 wt.%). The results are close to N-DES catalyst, where similar conversion was reported but within 10 min under identical conditions [13]. The identification of comparable optimum conditions for both systems enables a direct comparison of catalytic performance, ensuring that differences observed in subsequent sections arise from catalyst properties rather than variations in reaction conditions.

3.2 | Comparative Kinetics Analysis

Reaction kinetics were analyzed to provide comparative insight into the rate behavior of glycerolysis catalyzed by the phosphonium-based DES (P-DES), relative to the ammonium-based benchmark (N-DES), under identical reaction conditions. The objective of this analysis is not kinetic optimization, but to contextualize observed stability and recyclability trends in terms of apparent reaction rates.

TABLE 2 | Apparent activation energies (E_A) for glycerolysis catalyzed by phosphonium- and ammonium-based DESs.

Catalyst loading %	P-DES, E_A, KJ/mol	[a]N-DES, E_A, KJ/mol
1	84.79 ± 9.64	64.52 ± 9.56
5	80.23 ± 12.73	55.72 ± 7.49
10	40.33 ± 6.35	16.18 ± 2.23

[a]N-DES data adapted from [14] under identical conditions.

Given the large excess of glycerol employed, glycerolysis of oleic acid was treated using a pseudo-first-order kinetic approximation with respect to oleic acid concentration. The complete kinetic formulation, assumptions, and derivations are provided in Section S3.2. Apparent pseudo-first-order rate constants (k') were extracted from time-dependent conversion data obtained at different temperatures and catalyst loadings. Arrhenius plots of $\ln(k')$ versus temperature ($1/T$) were used to estimate apparent activation energies (E_A) for P-DES at catalyst loadings of 1–10 wt.% (Figure S3, Table 2). The calculated E_A decrease with increasing catalyst concentration, from approximately 85 kJ mol^{-1} at 1 wt.% to ~40 kJ mol^{-1} at 10 wt.%. The associated uncertainties in E_A arise primarily from regression fitting over limited temperature ranges and should therefore be interpreted qualitatively rather than as intrinsic kinetic constants. For comparison, Table 2, also list previously reported E_A trend for N-DES, under identical reaction conditions. It is observed that across catalyst loading, N-DES consistently has lower E_A than P-DES, corresponding to faster reaction rates reaching equilibrium conversion earlier (10 min) than P-DES (15 min).

The kinetic data, further validated optimal the catalyst dosage (10 wt.%) at 130°C and 15 min. These conditions were adopted here onwards for examining the effect of HBA substitution on catalyst performance, specifically recyclability.

FT-IR ATR analysis of biphasic products (fatty and aqueous) was done to verify the presence of glycerides and P-DES. Verification of esters formation in Section S3.2.1, provides comprehensive FT-IR spectrums (Figures S4 and S5) and associated analysis for neat oleic acid, P-DES and post-reaction fatty and aqueous (glycerol) phase. It was confirmed that glycerides made majority of fatty phase, while P-DES remained in aqueous phase, post reaction. The catalyst retention in aqueous phase is consistent with N-DES, suggesting hydrophilic nature of both DESs.

18673899, 2026, 11, Downloaded from https://chemistry-europe.onlinelibrary.wiley.com/doi/10.1002/cctc.70844 by James Cook University, Wiley Online Library on [10/11/2026]. See the Terms and Conditions (https://onlinelibrary.wiley.com/terms-and-conditions) on Wiley Online Library for rules of use; OA articles are governed by the applicable Creative Commons License

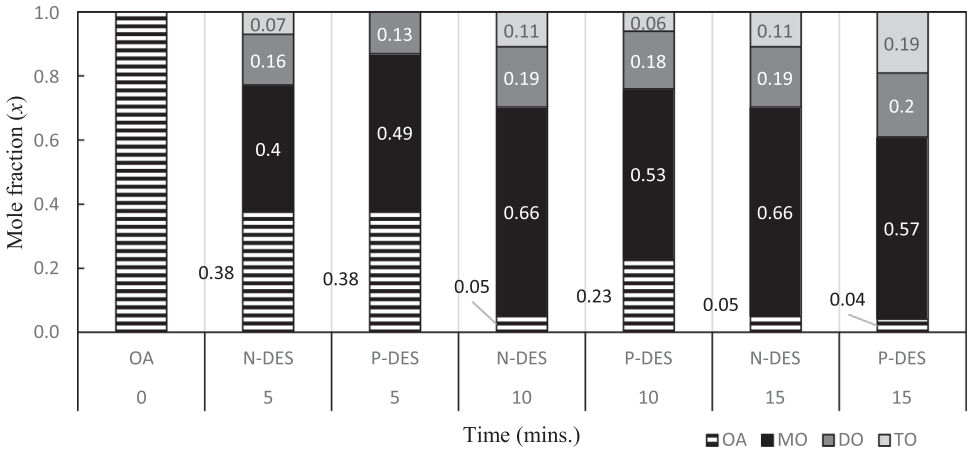


FIGURE 2 | Comparative change in the molar composition of the fatty phase with respect to time, data for N-DES adapted from [14].

The evolving product distribution during reaction is presented in Figure 2, for both DESs at optimized conditions. It is observed that the reaction proceeds via combination of parallel as well as consecutive pathways, producing mixture of glycerides during the reaction. Rapid formation of monoglycerides and gradual formation of di- and tri-glycerides is observed. N-DES shows faster monoolein accumulation and subsequent product stabilization, consistent with its lower E_A. While, P-DES shows a more gradual monoolein accumulation and subsequent transformations, in accordance with its higher E_A. At lower temperatures or catalyst loadings, similar qualitative trends are expected, with delayed progression toward higher glycerides due to kinetic limitations. The underlying acid-catalyzed esterification mechanism is well established for DES-mediated glycerolysis systems and has been reported previously for ammonium-based DES catalysts; therefore, it is not repeated here.

3.3 | Catalyst Stability and Recyclability

Evidence generated in the present study reveals that water is the immediate cause limiting equilibrium conversion, as aggressive through-volume N_2 purging for in situ water-removal increased P-DES catalyzed equilibrium conversion from ~94% to near-completed conversion ~99.4% (Figure S6 and S3.3.1). This behavior closely parallels that reported previously for the ammonium-based DES system (N-DES ≈ 98.8% under analogous purging conditions [14]), supporting the conclusion that water accumulation constrains equilibrium conversion in both catalyst systems.

Further, recyclability of P-DES is examined and compared with the ammonium benchmark under an identical handling regime: practical post-reaction oven-evaporation (105°C) water removal between cycles. After each run the organic and glycerol layers were separated by gravity (Figure S7), the glycerol phase was topped up with fresh glycerol to restore reactant molar ratio. The recovered glycerol phase (with or without oven treatment) was reused for the next cycle. Full experimental details for the recyclability protocol, mass-balance tracking, and make-up glycerol additions are provided in Tables S2–S4.

Figure 3a shows oleic acid conversion for both DESs, for five consecutive runs. For N-DES, the catalytic conversion drops from 94% in fresh run to ~40% in fifth run, showcasing substantial loss of catalytic activity. For P-DES, the results are similar, where P-DES performs marginally better, with 46% conversion at the end of fifth cycle. Table S2 shows water content in upper and lower layers of biphasic products, measured before starting the reaction. It can be seen that there is consistent water accumulation in recycled lower glycerol layer. The accumulating water limits equilibrium conversion, and also may be affecting P-DES structurally. Figure 3b shows the oleic acid conversion profile for both DESs, when lower glycerol layer was subjected to overnight oven evaporation (105°C) for removing water, before each recycle run. Table S3 shows mass lost during evaporation, presumably mostly water. Water removal has a pronounced effect on catalyst recyclability. For both DESs, the consecutive runs show increased oleic acid conversions, where the gap between both DESs widens. P-DES now shows superior catalytic activity with gradual reduction in OA conversion, while for N-DES there is a sudden loss in catalytic conversion. P-DES retains ≈ 81% conversion after five cycles, compared with ≈ 62.5% for N-DES. These results reconfirm that water is a deterioration agent in glycerolysis reaction limiting equilibrium conversion as well as a DES performance disruptor.

To exclude simple material-handling artefacts as the cause of conversion loss, mass-balance tracking was performed during the recyclability campaign (Table S4). Transfer-related losses of the glycerol phase (measured W_{LL}) were small and non-accumulative and could not account for the large decline in conversion observed without water removal; make-up glycerol additions (W_{MUG}) restored the nominal charge between cycles. These data therefore indicate that conversion decline is dominated by chemical/solvation effects (water accumulation and its consequences for the catalytic microenvironment) rather than by gross physical loss of catalyst during handling.

Thermogravimetric analysis (TGA, Figure S1) confirms that both N-DES and P-DES catalysts are thermally stable within the operable temperature range employed in this study (≤ 130°C), with no evidence of abrupt decomposition under reaction or oven-evaporation conditions. Thermal degradation can therefore be excluded as the origin of the observed differences in catalyst recyclability. Hammett acidity (H_0) measurements (Figure 4) establish that both DESs possess strong Brønsted acidity, consis-

18673899, 2026, 11, Downloaded from https://chemistry-europe.onlinelibrary.wiley.com/doi/10.1002/cctc.70844 by James Cook University, Wiley Online Library on [10/11/2026]. See the Terms and Conditions (https://onlinelibrary.wiley.com/terms-and-conditions) on Wiley Online Library for rules of use; OA articles are governed by the applicable Creative Commons License

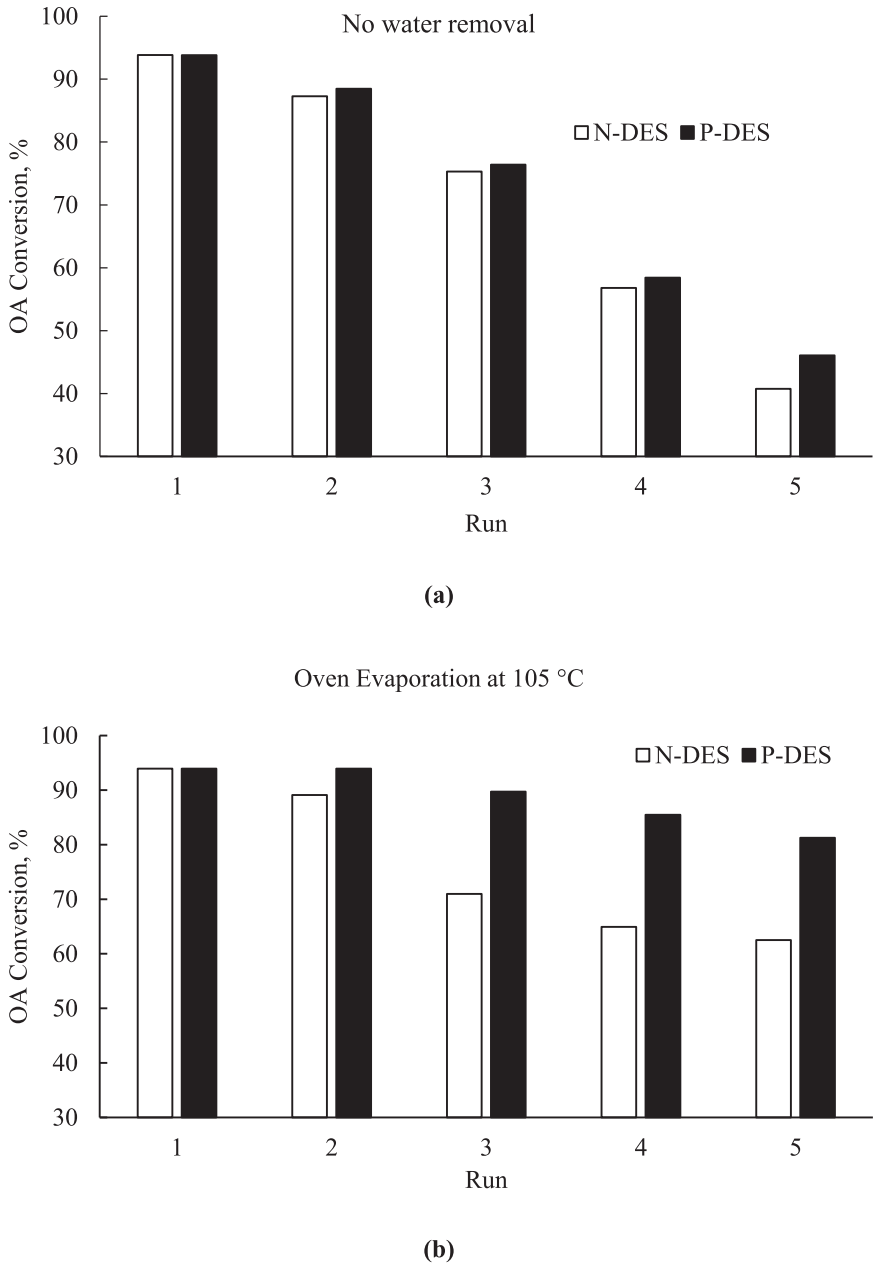


FIGURE 3 | Catalyst recyclability under repeated glycerolysis cycles. (a) Recyclability of P-DES and N-DES deep eutectic solvent catalysts over five consecutive cycles without any water-removal step between runs. (b) Recyclability of P-DES and N-DES catalysts over five consecutive cycles with oven-assisted water removal (105°C) between runs.

tent with their high catalytic activity in glycerolysis. The higher apparent acidity of the N-DES correlates with its lower apparent E_A (Table 2) and faster attainment of equilibrium conversion (≈ 10 min for N-DES versus ≈ 15 min for P-DES under otherwise identical conditions). H_0 measurements performed over a range of aqueous DES concentrations (10–40 mM) capture the influence of dilution and solvation on proton activity. These results provide a useful framework for interpreting effective acidity under varying catalyst loadings in the present biphasic system, where direct in situ measurement is not well-defined. However, acidity alone does not explain the superior recyclability of P-DES. Instead, the enhanced operational durability of P-DES is interpreted to arise, at least in part, from higher dynamic viscosity at reaction temperatures (Figure 5), which influences the catalyst microenvironment within the glycerol phase. Additionally, the higher viscosity of P-DES may also be linked to higher E_A, as high viscosity imposes greater mass-transfer limitations in the studied biphasic glycerolysis reaction, especially at lower reaction temperatures. Furthermore, increased viscosity may reduce catalyst mobility and mitigate adverse water-induced solvation effects, which may contribute to stabilization of protonic catalytic sites during repeated cycling. These physical effects may become particularly important under water-rich reaction conditions (recycle runs), where P-DES retains higher activity than the more kinetically active but less durable ammonium analogue. Relationships between viscosity, molecular mobility, and transport behavior in DES systems have been widely reported, with higher viscosity often associated with reduced diffusivity

18673899, 2026, 11, Downloaded from https://chemistry-europe.onlinelibrary.wiley.com/doi/10.1002/cctc.70844 by James Cook University, Wiley Online Library on [10/11/2026]. See the Terms and Conditions (https://onlinelibrary.wiley.com/terms-and-conditions) on Wiley Online Library for rules of use; OA articles are governed by the applicable Creative Commons License

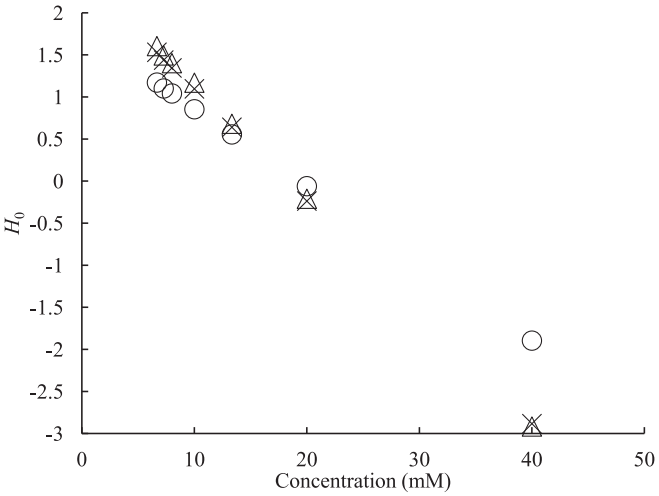


FIGURE 4 | Hammett acidity for studied DESs at different aqueous concentrations, reproduced from [13]. Δ: N-DES, O: P-DES, and X: PTSAM.

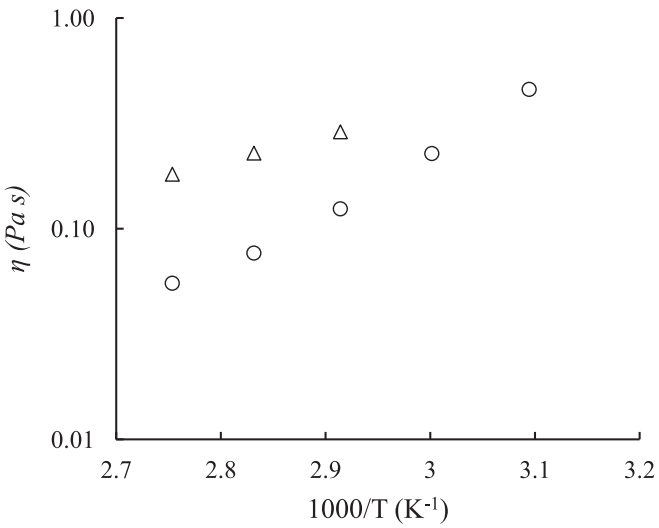
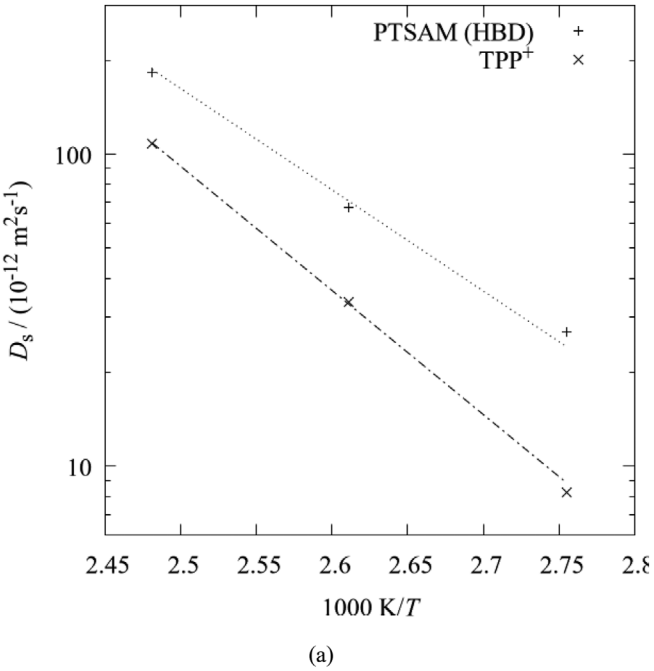


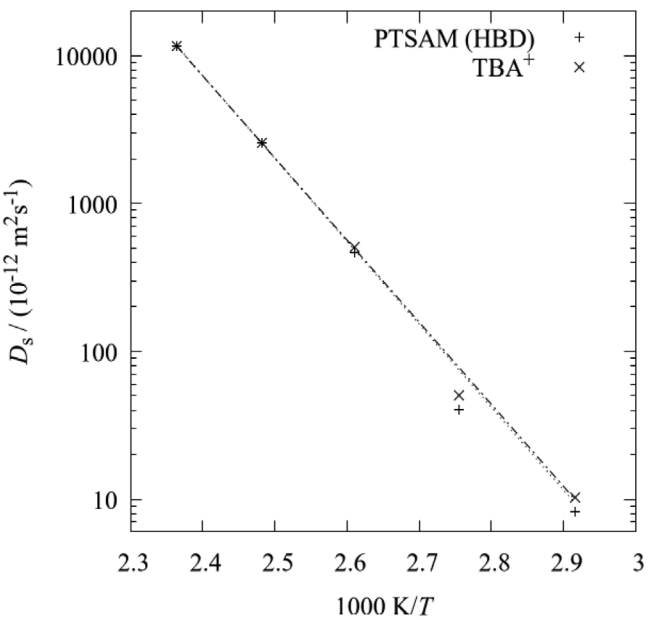
FIGURE 5 | Dynamic viscosity (η), vs. temperature ($1/T$) for DESs. O: N-DES, Δ: P-DES. Reproduced from [13].

and altered local structuring [18]. While direct in situ characterization of the DES microenvironment under reaction conditions would be challenging, the H_0, viscosity and recyclability data are collectively consistent with this interpretation.

A further scientific rationale behind differing catalyst recyclability can be developed based on previously reported ^{1}H-NMR self-diffusion studies (Figure 6) [13]. Briefly, in N-DES, ammonium cation (TBA^+) and HBD diffuse at comparable rates suggesting strongly associated H-bond network. While in P-DES, the HBD diffuses faster than the phosphonium cation (TPP^+) suggesting partial component decoupling. From this structural distinction, it can be inferred that HBD in P-DES retains greater mobility within a more dynamic and reorganizable H-bond network, whereas in more tightly associated N-DES, such mobility is rather restricted. As a result, the N-DES structure is more susceptible to water ingress during repeated recycling. Moreover, TPP^+ cation consists of aromatic substituents and exhibits greater charge delocalization, which may reduce ion pairing and weaken DES hydrogen-bond network strength, in comparison to TBA^+ analogue. Such moderation may lead to less tightly associated liquid structure, consistent with NMR diffusion observations. As such, in P-DES system, the microstructure may adapt under hydration–drying perturbation, suggesting improved resilience to disruption by water. These molecular-level differences are fully consistent with the observed trade-off between catalytic activity and operational durability identified in the present recyclability study.



(a)



(b)

FIGURE 6 | Arrhenius plots of the self-diffusion coefficients for the respective cation species and common HBD in synthesized DESs; (a) N-DES (343–423 K), (b) P-DES (363–403 K). Reproduced from [13].

18673899, 2026, 11, Downloaded from https://chemistry-europe.onlinelibrary.wiley.com/doi/10.1002/cctc.70844 by James Cook University, Wiley Online Library on [10/11/2026]. See the Terms and Conditions (https://onlinelibrary.wiley.com/terms-and-conditions) on Wiley Online Library for rules of use; OA articles are governed by the applicable Creative Commons License

Such decoupling of molecular motion and deviations from simple transport models have been observed in a range of DES systems, where translational and rotational dynamics reflect the underlying hydrogen-bond network organization rather than simple ionic behavior [19, 20]. Pulsed-field gradient NMR studies of choline chloride-based DESs have similarly shown unequal diffusion of HBA and HBD components, including in reline (ChCl:Urea), where diffusion asymmetry has been interpreted as reflecting underlying differences in component association and network organization rather than instability of the solvent structure [21]. This interpretation is further supported by reports that hydrated DESs, specifically reline retain nano-structural organization over substantial water contents before transitioning toward simple aqueous solutions, demonstrating that hydrogen-bonded DES networks can remain functionally resilient under water ingress [22]. Recent studies further demonstrate that DES structure and stability are highly sensitive to environmental conditions, including water incorporation and temperature, which can influence hydrogen-bond connectivity and system behavior [23]. By analogy, the P-DES investigated here may exhibit a similarly water-responsive yet structurally persistent catalytic environment.

Taken together, the acidity, viscosity, self-diffusion, and recyclability results support the hypothesis that HBA substitution influences catalyst durability primarily through modifications to DES microstructure, component mobility, and water response, rather than through changes in intrinsic acidity alone.

4 | Conclusion

Earlier work on N-DES catalyzed glycerolysis identified accumulation of water in the glycerol phase as a major factor limiting equilibrium conversion and undermining catalyst reuse. The present work examines whether phosphonium-HBA substitution alters this failure mode: specifically, whether phosphonium-based DES (P-DES) shows comparable water sensitivity, and whether its physicochemical profile confers improved operational durability under practical recycle handling, in glycerolysis of FFAs.

Tested under controlled reaction parameter range, both DESs proved efficient acidic catalysts. Both DESs exhibit strong Bronsted acidity, with differing dynamic viscosity and component mobility. Critically, P-DES exhibits higher dynamic viscosity at reaction temperatures and ^{1}H-NMR self-diffusion data show partial decoupling of the acidic HBD (PTSAM) from the phosphonium cation, whereas in N-DES the cation and PTSAM diffuse together. These observations support the interpretation that P-DES provides a more viscous and dynamically adaptable acidic microenvironment, in which Brønsted acid sites remain functionally available despite water-induced perturbations to the hydrogen-bond network, thereby improving durability at the expense of reaction rate. Comparative physicochemical analysis indicates that these differences arise primarily from changes in component mobility influencing DES microstructure and thus, water response introduced by HBA substitution, rather than differences in intrinsic acidity or thermal stability. These findings identify HBA identity as a practical catalyst-design variable for tuning the balance between reaction rate and durability in homogeneous DES catalysts.

One key limitation of present work is its focus on a single pair of HBA chemistries. Future works should focus on developing advanced probing techniques to investigate water-induced disruption of catalytic microenvironment. A key takeaway of current work is the critical need to explore effective water removal strategies when working with DES-based systems. Essentially, there is a need to extend the HBA substitution concept across broader DES families to validate structure-stability-performance relationships identified here.

Acknowledgments

We acknowledge the New Zealand Government through the Ministry of Foreign Affairs and Trade (MFAT) for providing New Zealand Development Scholarships. We also acknowledge Dr Matthew Sidford, Technical Manager, Chemical and Materials Engineering department, The University of Auckland, for his support with analytical measurements throughout this study. We also acknowledge Raymond Hoffmann (Senior Technician), Chemical and Materials Engineering department, The University of Auckland, for his support with fabrication of the reaction vessel and associated auxiliaries.

Open access publishing facilitated by The University of Auckland, as part of the Wiley - The University of Auckland agreement via the Council of Australasian University Librarians

Conflicts of Interest

The authors declare no conflicts of interest.

Data Availability Statement

The data that support the findings of this study are available in the Supporting Information of this article.

References

1. M. Ali Ijaz Malik, S. Zeeshan, M. Khubaib, et al., "A Review of Major Trends, Opportunities, and Technical Challenges in Biodiesel Production From Waste Sources," *Energy Conversion and Management: X* 23 (2024): 100675, https://doi.org/10.1016/j.ecmx.2024.100675.

2. R. T. Alarcon, G. I. Dos Santos, C. Gaglieri, A. De Moura, C. ÉTG, and G. Bannach, "Lipidic Biomass as a Renewable Chemical Building Block for Polymeric Materials," *Chemical Communications* 60 (2024): 14557–14572, https://doi.org/10.1039/D4CC04993D.

3. E. Aguilar-Garnica, F. Rodríguez-Palomera, J. P. García-Sandoval, and F. M. E. Escalante, "Dynamical Modeling for Biodiesel Production From Grease Trap Wastes," *Chemical Engineering Science* 117 (2014): 396–406, https://doi.org/10.1016/j.ces.2014.07.006.

4. A. Hayyan, M. A. Hashim, and M. Hayyan, "Agro-Industrial Acidic Oil as a Renewable Feedstock for Biodiesel Production Using (1R)-(–)-Camphor-10-Sulfonic Acid," *Chemical Engineering Science* 116 (2014): 223–227, https://doi.org/10.1016/j.ces.2014.03.031.

5. A. Ribeiro, F. Castro, and J. Carvalho, "Influence of Free Fatty Acid Content in Biodiesel Production on Non-Edible Oils," *WASTES: Solutions, Treatments and Opportunities* (2011): 425–430.

6. K. Mamtani, K. Shahbaz, and M. M. Farid, "Glycerolysis of Free Fatty Acids: A Review," *Renewable and Sustainable Energy Reviews* 137 (2021): 110501, https://doi.org/10.1016/j.rser.2020.110501.

7. K. Mamtani, K. Shahbaz, and M. M. Farid, "Deep Eutectic Solvents—Versatile Chemicals in Biodiesel Production," *Fuel* 295 (2021): 120604, https://doi.org/10.1016/j.fuel.2021.120604.

18673899, 2026, 11, Downloaded from https://chemistry-europe.onlinelibrary.wiley.com/doi/10.1002/cctc.70844 by James Cook University, Wiley Online Library on [10/11/2026]. See the Terms and Conditions (https://onlinelibrary.wiley.com/terms-and-conditions) on Wiley Online Library for rules of use; OA articles are governed by the applicable Creative Commons License

8. E. Guzmán, "Catalysis With Deep Eutectic Solvents: Challenges and Opportunities," *ChemCatChem* 17 (2025): e202500522, https://doi.org/10.1002/cctc.202500522.

9. S. E. Hooshmand, S. Kumar, I. Bahadur, T. Singh, and R. S. Varma, "Deep Eutectic Solvents as Reusable Catalysts and Promoter for the Greener Syntheses of Small Molecules: Recent Advances," *Journal of Molecular Liquids* 371 (2023): 121013, https://doi.org/10.1016/j.molliq.2022.121013.

10. E. L. Smith, A. P. Abbott, and K. S. Ryder, "Deep Eutectic Solvents (DESs) and Their Applications," *Chemical Reviews* 114 (2014): 11060–11082, https://doi.org/10.1021/cr300162p.

11. S. Shafique, A. S. Belousov, R. Rashid, et al., "Deep Eutectic Solvents (DES): Structure, Properties, and Cutting-Edge Applications in Green Catalysis," *Journal of Molecular Liquids* 419 (2025): 126769, https://doi.org/10.1016/j.molliq.2024.126769.

12. A. T. H. Yeow, A. Hayyan, M. Hayyan, and J. Saleh, "A Comprehensive Review on the Physicochemical Properties of Deep Eutectic Solvents," *Results in Chemistry* 7 (2024): 101378, https://doi.org/10.1016/j.rechem.2024.101378.

13. K. Mamtani, S. J. Stevenson, P. Galvosas, C. C. Weber, M. M. Farid, and K. Shahbaz, "Synthesis and Characterization of Acidic Deep Eutectic Solvents Based on p-Toluenesulfonic Acid," *Journal of Molecular Structure* 1294 (2023): 136378, https://doi.org/10.1016/j.molstruc.2023.136378.

14. K. Mamtani, M. M. Farid, and K. Shahbaz, "Application of Quaternary Ammonium-Based Deep Eutectic Solvents as Catalysts for the Glycerolysis of Free Fatty Acids," *Energy & Fuels* 37 (2023): 7848–7855, https://doi.org/10.1021/acs.energyfuels.3c00666.

15. Y. Marcus, *Deep Eutectic Solvents* (1st ed., Springer Cham, 2019), https://doi.org/10.1007/978-3-030-00608-2.

16. Lubrizol Advanced Materials, Inc. Test Procedure, TP-TM-001C: Determination of Acid Value and Free Fatty Acid; The Lubrizol Corporation, 2009.

17. S. T. Williamson, K. Shahbaz, F. S. Mjalli, I. M. AlNashef, and M. M. Farid, "Application of Deep Eutectic Solvents as Catalysts for the Esterification of Oleic Acid With Glycerol," *Renewable Energy* 114 (2017): 480–488, https://doi.org/10.1016/j.renene.2017.07.046.

18. A. González De Castilla, J. P. Bittner, S. Müller, S. Jakobtorweihen, and I. Smirnova, "Thermodynamic and Transport Properties Modeling of Deep Eutectic Solvents: A Review on G^E -Models, Equations of State, and Molecular Dynamics," *Journal of Chemical and Engineering Data* 65 (2020): 943–967, https://doi.org/10.1021/acs.jced.9b00548.

19. A. Schulz, K. Moch, Y. Hinz, P. Lunkenheimer, and R. Böhmer, "Translational and Reorientational Dynamics in Carboxylic Acid-Based Deep Eutectic Solvents," *Journal of Chemical Physics* 160 (2024): 074503, https://doi.org/10.1063/5.0189533.

20. A. Schulz, P. Lunkenheimer, and A. Loidl, "Rotational Dynamics, Ionic Conductivity, and Glass Formation in a $ZnCl_2$-Based Deep Eutectic Solvent," *Journal of Chemical Physics* 160 (2024): 054502, https://doi.org/10.1063/5.0187729.

21. C. D'Agostino, R. C. Harris, A. P. Abbott, L. F. Gladden, and M. D. Mantle, "Molecular Motion and Ion Diffusion in Choline Chloride Based Deep Eutectic Solvents Studied by 1H Pulsed Field Gradient NMR Spectroscopy," *Physical Chemistry Chemical Physics* 13 (2011): 21383, https://doi.org/10.1039/c1cp22554e.

22. O. S. Hammond, D. T. Bowron, and K. J. Edler, "The Effect of Water Upon Deep Eutectic Solvent Nanostructure: An Unusual Transition From Ionic Mixture to Aqueous Solution," *Angewandte Chemie International Edition* 56 (2017): 9782–9785, https://doi.org/10.1002/anie.201702486.

23. J. H. Yang, A. W. S. Ooi, Z. A. H. Goodwin, et al., "Room-Temperature Decomposition of the Ethaline Deep Eutectic Solvent," *Journal of Physical Chemistry Letters* 16 (2025): 3039–3046, https://doi.org/10.1021/acs.jpclett.4c03645.

Supporting Information

Additional supporting information can be found online in the Supporting Information section.

Supporting File: cctc70844-sup-0001-SuppMat.docx.

18673899, 2026, 11, Downloaded from https://chemistry-europe.onlinelibrary.wiley.com/doi/10.1002/cctc.70844 by James Cook University, Wiley Online Library on [10/11/2026]. See the Terms and Conditions (https://onlinelibrary.wiley.com/terms-and-conditions) on Wiley Online Library for rules of use; OA articles are governed by the applicable Creative Commons License